Control of Crystal Structure and Orientation of Ni(salen) by Epitaxial Growth on Alkali Halide

Kaname Yoshida* and Seiji Isoda

Institute for Chemical Research, Kyoto University, Uji, Kyoto 611 0011, Japan

Received July 17, 2007. Revised Manuscript Received October 6, 2007

Thin films of *N*,*N*′-bis(salicylaldehydo)ethylenediaminato nickel(II) (Ni(salen)) are fabricated by vacuum epitaxy on (001) surfaces of KBr, KCl, and NaCl substrates and characterized by transmission electron microscopy. Two new monoclinic polymorphs of Ni(salen), β ($a = 2.59$ nm, $b = 1.54$ nm, $c = 0.670$ nm, $\beta = 92.6°$) and γ ($a = 2.56$ nm, $b = 0.787$ nm, $c = 0.743$ nm, $\beta = 93.7°$), are successfully identified by electron diffractions and high resolution images. The β form is produced on all three substrates by deposition at room temperature, while the γ form is produced on NaCl and KCl at 90 °C. The orientation of these polymorphs is controlled by lattice matching. Although the γ form is energetically favorable with better lattice matching to these substrates, the faster-growing β form is preferentially produced at lower substrate temperature. The polymorphic structure of the deposited film is thus governed by both the substrate surface structure and the growth temperature.

Introduction

Certain transition-metal complexes with Schiff base ligands exhibit unusual electronic properties, such as high redox potential.[1–5] The electronic properties of such materials have been examined extensively in attempts to construct synthetic models of biological compounds like metalloproteins and metalloenzymes,[5–8] and it has been found that small changes to the ligand structure can substantially enhance or inhibit certain biological and/or catalytic responses of the complex.[9] Investigations of the redox potential of metal complexes with Schiff bases have generally been conducted in solution using electrochemical techniques.[1–6,10] However, the electronic properties of these materials in the solid phase are dependent not only on the molecular behavior but also on the effect of crystal structures, which modulate intermolecular interactions. Information on the structure in solid form is considered essential for developing novel applications of the useful electronic properties of Schiff base complexes. In this sense, the design of molecular packing is as important as the design of molecules in achieving specific intermolecular interactions.

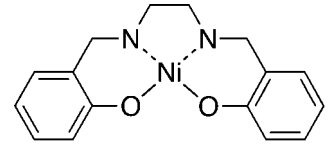

Figure 1. Chemical structure of Ni(salen).

In the present paper, the formation mechanisms of polymorphs in epitaxial thin films of *N*,*N*′-bis(salicylaldehydo)ethylenediaminato nickel(II) (Ni(salen)) grown on single-crystalline alkali halide substrates by vacuum deposition are investigated in detail. Ni(salen) is a tetradentate Schiff base complex in which the central nickel atom sits in a plane-square environment coordinating two nitrogen and two oxygen atoms of the ligand (Figure 1). Ni(salen) has been used for catalytic reactions,[11,12] for redox polymerization,,[13–15] and as a gas sensor[16] yet does not appear to have been applied as an epitaxial thin film. Epitaxial growth on suitable crystalline substrates allows for strict control of molecular packing,[17–19] potentially leading to the discovery of a new polymorph with new or improved functionality. Single crystals of Ni(salen)

* To whom correspondence should be addressed. Telephone: +81-774-38-3052. Fax: +81-774-38-3055. E-mail: yoshida@eels.kuicr.kyoto-u.ac.jp.

(1) Araya, L. M.; Vargas, J. A.; Costamagna, J. A. *Transition Met. Chem.* **1986**, *12*, 312–316.
(2) Gili, P.; Martin Reyes, M. G.; Martin Zarza, P.; Guedes da Silva, M. F. C.; Tong, Y.-Y.; Pombeiro, A. J. L. *Inorg. Chim. Acta* **1997**, *255*, 279–288.
(3) Hotchandani, S.; Ozdemir, U.; Nasr, C.; Allakhverdiev, S. I.; Karacan, N.; Klimov, V. V.; Kamat, P. V.; Carpentier, R. *Bioelectrochem. Bioenerg.* **1999**, *48*, 53–59.
(4) Szlyk, E.; Biniaka, S.; Larsen, E. J. *Solid State Electrochem.* **2001**, *5*, 221–226.
(5) Taylor, M. K.; Stevenson, D. E.; Berlouis, L. E. A.; Kennedy, A. R.; Reglinski, J. J. *Inorg. Biochem.* **2006**, *100*, 250–259.
(6) Patterson, G. S.; Holm, R. H. *Bioinorg. Chem.* **1975**, *4*, 257–275.
(7) Sreenivasulu, B.; Zhao, F.; Gao, S.; Vittal, J. J. *Eur. J. Inorg. Chem.* **2006**, *2006*, 2656–2670.
(8) Mirkhani, V.; Moghadam, M.; Tangestaninejad, S.; Bahramian, B.; Mallekpoor-Shalamzari, A. *Appl. Catal., A* **2007**, *321*, 49–57.
(9) Constamagna, J.; Vargas, J.; Latorre, R.; Alvarado, A.; Mena, G. *Coord. Chem. Rev.* **1992**, *119*, 67–88.
(10) Sakurai, T.; Hongo, J.; Nakahara, A. *Inorg. Chim. Acta* **1980**, *46*, 205–210.
(11) Lim, L. F.; Cardozo-Filho, L.; Arroyo, P. A.; Márquez-Alvarez, H.; Antunes, O. A. C. *React. Kinet. Catal. Lett.* **2005**, *84*, 69–77.
(12) Chatterjee, D.; Bajaj, H. C.; Das, A.; Bhatt, K. J. *Mol. Catal.* **1994**, *92*, L235–L238.
(13) Shagisultanova, G. A.; Ardasheva, L. P. *Russ. J. Appl. Chem.* **2003**, *76*, 1626–1630.
(14) Shagisultanova, G. A.; Ardasheva, L. P.; Orlova, I. A. *Russ. J. Appl. Chem.* **2003**, *76*, 1631–1636.
(15) Tchepournaya, I.; Vasilieva, S.; Logvinov, S.; Timonov, A.; Amadelli, R.; Bartak, D. *Langmuir* **2003**, *19*, 9005–9012.
(16) Mao, L. Q.; Tian, Y.; Shi, G. Y.; Liu, H. Y.; Jin, L. T.; Yamamoto, K.; Tao, S.; Jin, J. Y. *Anal. Lett.* **1998**, *31*, 1991–2007.

10.1021/cm7018789 CCC: $37.00
Published on Web 11/13/2007

recrystallized from acetone are known to have an orthorhombic structure involving dimeric Ni(salen),[20,21] referred to hereafter as the α form; orthorhombic, $a = 1.3831$ nm, $b = 2.6155$ nm, and $c = 0.7482$ nm. The crystallographic structures and orientations of Ni(salen) thin films fabricated in this study are characterized by microscopic analyses and compared to this α form.

Experimental Details

Thin Films Fabrication. Ni(salen) films were grown by vacuum deposition onto freshly cleaved (001) surfaces of KBr, KCl, and NaCl. The substrate was heated to 400 °C in a vacuum chamber immediately prior to film deposition to eliminate contaminants on the substrate surface. The substrate temperature was maintained at room temperature (25 °C) or 90 °C during deposition, under a vacuum of approximately 1×10^{-5} Pa. The deposition rate was controlled with the aid of a quartz microbalance to a constant 1 nm/min, and the deposition was stopped once the films reached an average thickness of 20 nm.

Analysis of Structures and Epitaxial Relationships. The morphology of the Ni(salen) thin films was determined by atomic force microscopy (AFM, NanoScope IIIa, Digital Instruments), and the crystallographic orientations were measured by high-resolution electron diffraction (HRED) using a transmission electron microscope (JEM200CX, JEOL) at an acceleration voltage of 200 kV and a probe spot of several hundred micrometers in diameter. Samples for HRED observations were prepared by dissolving the alkali halide substrate on a water surface after reinforcing the film with a film of amorphous carbon. Unit cell parameters were determined by selected-area electron diffraction (SAED) using another transmission electron microscope (JEM2000FX-II, JEOL) and X-ray diffractometer (RAD-IIB, Rigaku). High-resolution transmission electron microscopy (HRTEM) images were captured using a cryogenic instrument (JEM4000SFX, JEOL) with a helium-cooled stage (4.2 K) at an acceleration voltage of 400 kV and compared with simulated ones as supporting information on molecular packing. At cryogenic temperatures, the stability of organic materials under electron irradiation is extended, allowing detailed observation of the molecular structures. Irradiation damage to specimens by the electron beam was minimized by employing a minimum dose system with photographic film.[22] Molecular packing of new polymorph structures were estimated by the comparison between the experimental HRTEM image and the simulated images calculated from model structures. To construct model structures, Ni(salen) molecules were arranged in the unit cells manually so as for each molecule not to interfere. Simulation of HRTEM image was achieved using software (MacTempas) based on a multislice method.

Results and Discussion

Orientation and Crystal Structure of Ni(salen) Films. All Ni(salen) films fabricated in this work were confirmed to have grown epitaxially on the alkali halide substrate.

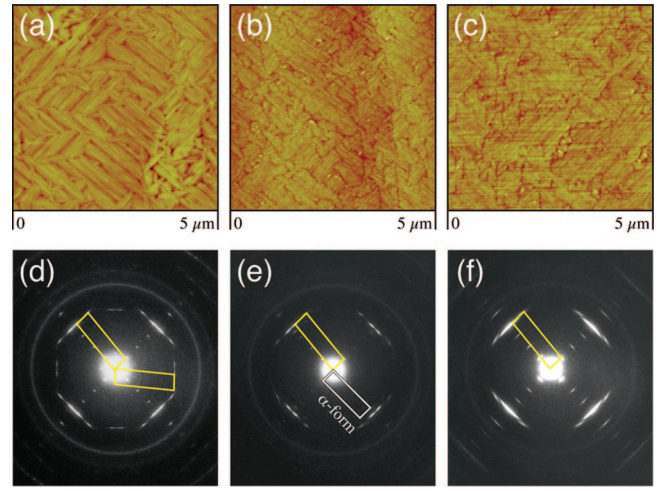

Figure 2. (a−c) AFM images and (d−f) HRED patterns of Ni(salen) films fabricated at 25 °C. Vertical and horizontal directions are subparallel to the [100] direction of the substrate. (a, d) KBr, (b, e) KCl, (c, f) NaCl. Quadrilaterals in HRED define the 2D primitive unit of the β (yellow) and α (white) forms.

Figure 2 shows AFM images and HRED patterns of the films grown at 25 °C. These films consist of needle-like crystals of Ni(salen) with long axes aligned parallel to the [110] direction of the substrate. On the KBr substrate, however, an appreciable fraction of the needle population is also oriented parallel to the [100] direction of the substrate (see Figure 2(d)). These HRED patterns are not in accord with the known orthorhombic α form, indicating the existence of a new polymorph structure, labeled here as the β form. The quadrilaterals in the HRED pattern define a tentative two-dimensional (2D) primitive unit cell of the β form (0.335 nm × 1.29 nm). Because of the fourfold symmetry of the substrate surface, the HRED patterns consist of multiple diffraction net patterns, despite being crystallographically a single-orientation film. As the short and long axes of the 2D unit cell of the β form crystallites are nearly parallel to the [110] direction of the substrate, the crystallographic direction of a needle crystal could not be determined solely from the HRED pattern. In addition to SAED, HRTEM could indicate that the needle axis corresponds to the short axis of the β form. The film on NaCl produces arcing diffraction spots in the HRED pattern as readable especially from the zeroth layer diffraction, suggesting a comparatively low degree of orientation in the β form on this substrate. A small amount of α-form crystals was identified on KCl, with b and c axes oriented parallel to the [110] direction of the substrate surface; the molecules stand their planes perpendicular to the substrate surface.

The morphology of Ni(salen) films grown at 90 °C differs substantially from that of those grown at room temperature. Figure 3 shows AFM images and HRED patterns of the films grown at 90 °C. The AFM images reveal dendrite-like crystals on KCl and NaCl and needle-like crystals of the β form on KCl and KBr. The HRED patterns for the dendrite-like crystals indicate another polymorphic structure differing from both the α and the β forms, labeled here as the γ form. The axes of the 2D unit cell of the γ form are aligned parallel to the [110] direction of NaCl and KCl. Thus, the film on

(17) Yoshida, K.; Yaji, T.; Koshino, M.; Isoda, S. J. *Jpn. Appl. Phys.* **2005**, *44*, 491–494.
(18) Yoshida, K.; Isoda, S.; Nemoto, T.; Kobayashi, T.; Sato, N.; Shirotani, I. *Mol. Cryst. Liq. Cryst.* **2000**, *342*, 121–126.
(19) Moulin, J.-F.; Brinkmann, M.; Thierry, A.; Wittmann, J.-C. *Adv. Mater.* **2002**, *14*, 436–439.
(20) Shkol'nikova, L. M.; Yumal', E. M.; Shugam, E. A.; Voblikova, V. A. J. *Struct. Chem.* **1970**, *11*, 819–823.
(21) Gaetani Manfredotti, A.; Guastini, C. *Acta Crystallogr.* **1983**, *C39*, 863–865.
(22) Fujiyoshi, Y.; Mizusaki, T.; Morikawa, K.; Yamagishi, H.; Aoki, Y.; Kihara, H.; Harada, Y. *Ultramicroscopy* **1991**, *38*, 241–251.

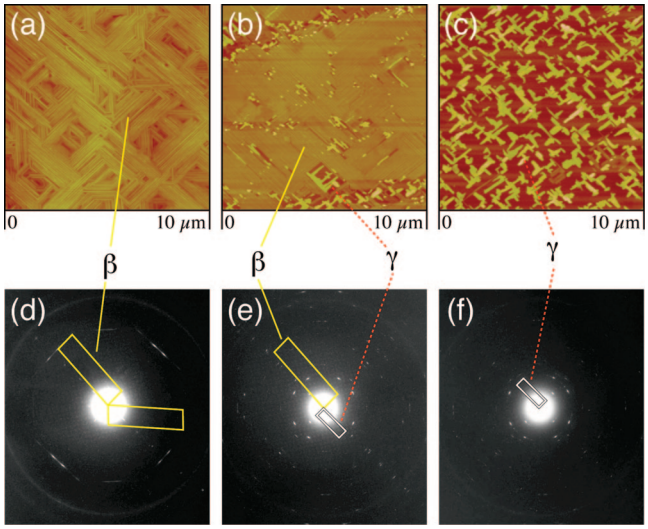

Figure 3. (a−c) AFM images and (d−f) HRED patterns of Ni(salen) films fabricated at 90 °C. Vertical and horizontal directions are subparallel to the [100] direction of the substrate. (a, d) KBr, (b, e) KCl, (c, f) NaCl. Quadrilaterals in HRED define the 2D primitive unit of the β (yellow) and γ (white) forms.

Table 1. Forms Grown on Each Substrate at 25 and 90 °C

	substrate temperature	
substrate	25 °C	90 °C
KBr	β [110][a], β [100][b]	β [110][a], β [100][b]
KCl	β [110][a], α [110][c]	β [110][a], γ [110][d]
NaCl	β [110][a]	γ [110][d]

[a] Needle axis of β form is parallel to the [110] direction of the substrate. [b] Needle axis of β form is parallel to the [100] direction of the substrate. [c] The b and c axes of α form are parallel to the [110] direction of the substrate. [d] The a and b axes of γ form are parallel to the [110] direction of the substrate.

KCl consists of both the β and the γ forms, while only the β form was present on KBr and only the γ form (2.56 nm × 0.787 nm) was found on NaCl. The forms grown on each substrates are summarized in Table 1.

Structural Analyses of β-Ni(salen) and γ-Ni(salen). The domain size of the β form is too small to allow acquisition of a single diffraction net pattern by SAED with the smallest area-selecting aperture used. The cell dimensions of the β form were thus determined by fast Fourier transform (FFT) analysis of the HRTEM image. Figure 4 shows a typical HRTEM image and the corresponding FFT pattern. The FFT pattern clearly shows a single net pattern, from which the β form can be determined to be an oblique unit with projected dimensions of 0.335 nm × 1.29 nm with an angle of 92.6°. Simulation of molecular packing for reconstruction of the three-dimensional (3D) unit cell indicates that the periodicities determined from the projected cell should be doubled because of the zigzag alignment of molecules along the c axis, giving unit cell dimensions of a = 2.59 nm, c = 0.670 nm, β = 92.6°, and b = 1.54 nm for the monoclinic β form (see Supporting Information). The ac-plane is parallel to the substrate surface so that the molecules stand perpendicular to the substrate surface. The molecular packing can be confirmed directly by analysis of HRTEM images. However, as the crystals of the Ni(salen) films are highly susceptible to beam damage, forcing the electron dose to

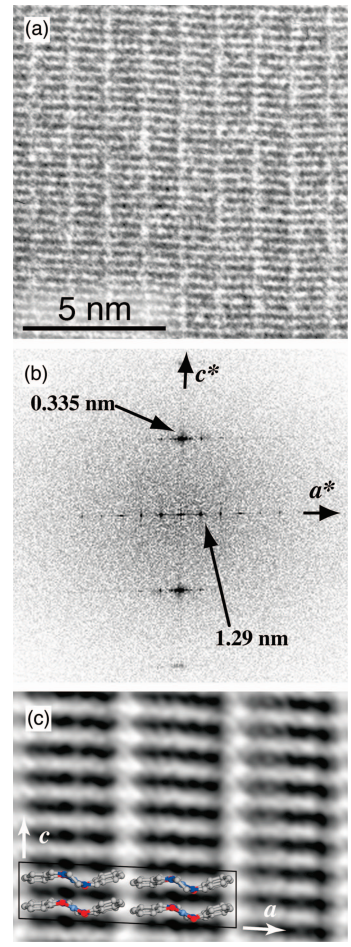

Figure 4. (a) HRTEM image of β-Ni(salen) and corresponding (b) 2D FFT and (c) filtered HRTEM image.

be minimized, the obtained HRTEM images were very noisy. Fourier filtering was thus applied to the raw HRTEM images to improve the signal-to-noise ratio and obtain improved molecular contrasts. The filtered HRTEM image and expected packing of the β form are shown in Figure 4c. This analysis confirms that the molecular column formed by lateral molecular packing is aligned along the c axis of the β structure, parallel to the [110] direction of substrate. Although precise molecular packings of new polymorphs were not decided because of the high degree of freedom including molecular conformations, an averaged intermolecular distance along the molecular column axis in the β structure could be shorter (~0.34 nm) than that in the α structure (~0.37 nm). So the intermolecular interaction in the β form could be larger than in the α form.

The 3D unit cell structure of the γ form was determined in a similar manner. Figure 5 shows SAED patterns of the γ form obtained by tilting specimens around the a^* axis with respect to the incident electron beam (0° corresponds to the incident beam parallel to the [001] direction of the γ form). Analysis of these SAED patterns in reference to X-ray diffraction data (see Supporting Information) gives unit cell dimensions of a = 2.56 nm, b = 0.787 nm, c = 0.743 nm, and β = 93.7° for the monoclinic γ form. The diffraction spots in the tilted SAED patterns consist of paired reflections in higher

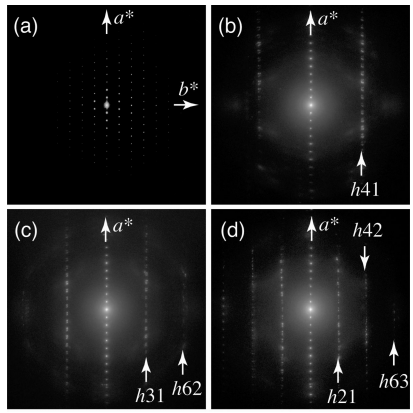

Figure 5. SAED patterns of γ-Ni(salen) at specimen tilts of (a) 0°, (b) 14.8°, (c) 19.4°, and (d) 27.7°.

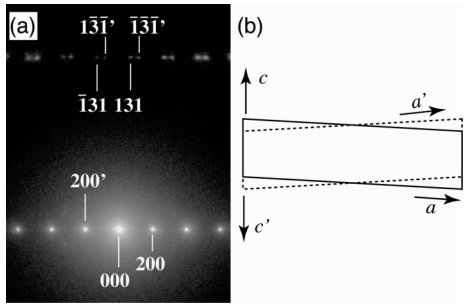

Figure 6. (a) Magnified SAED pattern of γ-Ni(salen) at 19.4° tilt. (b) Schematic drawing of crystallographic orientation of twinned γ-Ni(salen) projected along the [010] direction.

diffraction layers, attributable to the overlap of two net patterns from a twin structure symmetric with respect to the *bc* plane (see Figure 6b). Figure 7 shows an HRTEM image of the γ form and the corresponding FFT pattern and Fourier filtered HRTEM image. Considering the molecular packing (Figure 7c), we concluded that the molecular columns in the γ form are parallel to the *c* axis, close to perpendicular to the substrate surface. The averaged intermolecular distance along the molecular column in the γ and α structures is almost the same (~0.37 nm).

Origin of Ni(salen) Polymorphs. In determining the epitaxial orientation of the films, it is important to consider the misfit between the molecular structure of the film and the substrate surface structure, which affects the interfacial lattice energy in the point-on-line coincidence of epitaxial growth.[23–27] The lattice plane of the deposited crystal tends to be orientated parallel to the basic lattice line of the substrate surface when the lattice spacings are similar (i.e., small misfit). Misfit values are calculated for several lattice

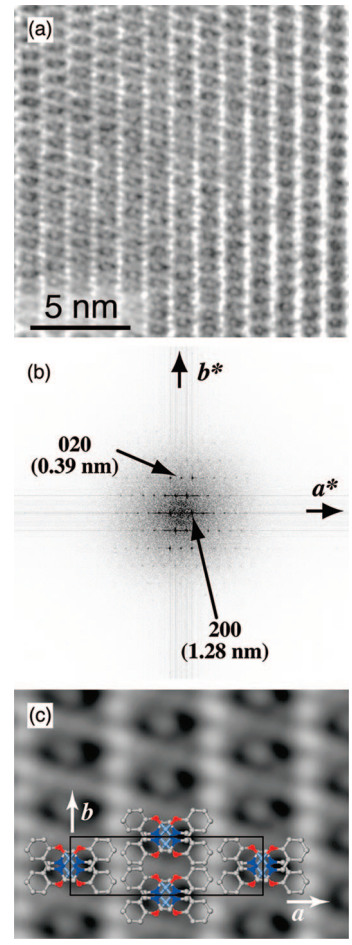

Figure 7. (a) HRTEM image of γ-Ni(salen) and corresponding (b) 2D FFT and (c) filtered HRTEM image.

Table 2. Misfit Values of γ-Ni(salen) on Various Substrates

	alkali halide *d* spacing	crystal possible *d* spacing	misfits
KBr		d_{500} = 0.512 nm	+9.6%
a = 0.660 nm	d_{110} = 0.467 nm	d_{600} = 0.427 nm	−8.6%
		d_{020} = 0.394 nm	−15.6%
KCl		d_{500} = 0.512 nm	+15.1%
a = 0.629 nm	d_{110} = 0.445 nm	d_{600} = 0.427 nm	−4.0%
		d_{020} = 0.394 nm	−11.5%
NaCl		d_{600} = 0.427 nm	+7.3%
a = 0.563 nm	d_{110} = 0.398 nm	d_{700} = 0.366 nm	−8.0%
		d_{020} = 0.394 nm	−1.0%

intervals of the Ni(salen) polymorphs and all substrates considered in this study by the following equation:

$$\text{misfit}(\%) = \frac{d_{\text{dep}} - d_{\text{sub}}}{d_{\text{sub}}} \times 100$$

where d_{sub} is the basic lattice spacing of the substrate surface and d_{dep} is the corresponding spacing of the deposited crystal. In most of the present cases, the (110) spacing of the substrate is assumed to correspond to that of the basic lattice, since the spacing corresponds to the lowest Fourier component of surface potential and the substrates were confirmed to have the [110] orientation. The (200) spacings of the substrate, the second-lowest Fourier component, are also considered where necessary. The results are tabulated in Tables 2–4. The cases with negative misfit are considered first for each substrate as observed by scanning tunneling

(23) Hoshino, A.; Isoda, S.; Kurata, H.; Kobayashi, T. J. *Appl. Phys.* **1994**, *76*, 4113–4120.
(24) Hoshino, A.; Isoda, S.; Kurata, H.; Kobayashi, T. J. *Cryst. Growth* **1995**, *146*, 636–640.
(25) Hoshino, A.; Isoda, S.; Kurata, H.; Kobayashi, T.; Yamashita, Y. *Jpn. J. Appl. Phys.* **1995**, *34*, 3858–3863.
(26) Fujiwara, E.; Isoda, S.; Ogawa, T.; Kobayashi., T.; Yamashita, Y. *Surf. Sci.* **2001**, *487*, 118–126.
(27) Fujiwara, E.; Isoda, S.; Hoshino, A.; Kobayashi, T.; Yamashita, Y. *Mol. Cryst. Liq. Cryst.* **2000**, *349*, 215–218.

Table 3. Misfit Values for β-Ni(salen) on Various Substrates

	alkali halide *d* spacing	crystal possible *d* spacing	misfits
KBr $a = 0.660$ nm	$d_{110} = 0.467$ nm	$d_{500} = 0.516$ nm	+10.5%
		$d_{600} = 0.430$ nm	−7.9%
	$d_{200} = 0.330$ nm	$d_{600} = 0.430$ nm	+30.3%
		$d_{800} = 0.323$ nm	−2.1%
KCL $a = 0.629$ nm	$d_{110} = 0.445$ nm	$d_{500} = 0.516$ nm	+16.0%
		$d_{600} = 0.430$ nm	−3.4%
	$d_{200} = 0.315$ nm	$d_{800} = 0.323$ nm	+2.5%
		$d_{1000} = 0.258$ nm	−18.1%
NaCl $a = 0.563$ nm	$d_{110} = 0.398$ nm	$d_{600} = 0.430$ nm	+8.0%
		$d_{700} = 0.368$ nm	−7.5%
	$d_{200} = 0.282$ nm	$d_{800} = 0.323$ nm	+14.5%
		$d_{1000} = 0.258$ nm	−8.5%

Table 4. Misfit Values for α-Ni(salen) on Various Substrates

	alkali halide *d* spacing	crystal possible *d* spacing	misfits
KBr $a = 0.660$ nm	$d_{110} = 0.467$ nm	$d_{050} = 0.523$ nm	+12.0%
		$d_{060} = 0.436$ nm	−6.7%
		$d_{002} = 0.374$ nm	−19.9%
KCl $a = 0.629$ nm	$d_{110} = 0.445$ nm	$d_{050} = 0.523$ nm	+17.6%
		$d_{060} = 0.436$ nm	−2.0%
		$d_{002} = 0.374$ nm	−15.9%
NaCl $a = 0.563$ nm	$d_{110} = 0.398$ nm	$d_{060} = 0.436$ nm	+9.5%
		$d_{070} = 0.374$ nm	−6.0%
		$d_{002} = 0.374$ nm	−6.0%

microscopy for monomolecular layers on substrate surfaces.[23–25] The positive misfit indicates that the unit cell of the deposited layer will be compressed at the interface to achieve complete point-online coincidence but is in general considered energetically unfavorable for deposited layers. The smallest negative misfit for each substrate is therefore expected to correspond to the realized epitaxial orientation. The lattice spacings of the γ form deposited at 90 °C match the NaCl and KCl lattices well, with a misfit of −1.0% and −4.0%, respectively (Table 2). At such high substrate temperature, the deposited molecules are able to migrate longer distances, allowing formation of the γ form whose lattice fits the NaCl and KCl surfaces better. The observed orientation of the γ form can be explained by this misfit. On KBr, however, there is no low negative value of the misfit for the γ form. Instead, the β form provides the best match to KBr: −7.9% misfit for the [110] orientation and −2.1% for the [100] orientation. This may explain the growth of just the β form on KBr, even at 90 °C. These relationships between the observed orientation and the theoretical misfit suggest the existence of a hypothetical threshold misfit value of approximately −8.0%. This threshold might depend on the elasticity of the deposited layers, which allows the lattice to distort to register correctly on the substrate lattice. The comparatively low misfit value of −3.4% for the β form on KCl would thus allow the β form to grow on KCl in addition to the γ form.

The two orientations of the β form grown on KBr at 25 °C can be similarly explained by the threshold misfits for both orientations (−7.9%, −2.1%). When this −8.0% threshold is used, a single orientation of the β form orientated parallel to the [110] direction can be expected for NaCl (misfit = −7.5%). However, the origin of arcing of the HRED pattern for NaCl is not clear at present. On KCl, the [110] orientations of the β and α forms have misfit values of −3.4% and −2.0%, respectively.

The formation of the β- and γ-form polymorphs of Ni(salen) appears to be dominant in the vapor-phase deposition of the present films. Metal−salen complexes are known to adopt several conformations, such as umbrella- and step-shaped conformations.[28] The most favorable structure for free Ni(salen) molecules is the step shape,[29] whereas the α form is known to consist of a dimeric pair of umbrella-shaped Ni(salen) molecules.[21] The nucleation rate of the α form from the vapor phase is thus considered to be slower than for the β and γ forms.

Inspection of Tables 2–4 indicates that the misfit alone is unable to explain the exclusive growth of the β and γ forms, as the misfits for the two forms are both below the threshold value determined above. For example, the misfits for the γ and β forms on NaCl are −1.0% and −7.5%, respectively (accounting for thermal expansion of the substrate), yet only the β form grew at 25 °C and only the γ form grew at 90 °C. Therefore, the polymorph formed in epitaxial growth appears to be directly influenced by the substrate temperature. Crystalline Ni(salen) powder obtained from an acetone solution by fast evaporation of the solvent includes both the α form and the β form, while only the β form is obtained by vapor-phase deposition on aperiodic amorphous carbon or glass substrates over a wide temperature range (see Supporting Information). This suggests that the growth of the β form is triggered by rapid crystallization rather than lattice match on a periodic surface. Thus, at low substrate temperature, which is characterized by relatively fast solidification, molecular columns of the β form grow preferentially, aligned parallel to the [110] direction of the substrate to satisfy lattice matching. The γ form is unable to nucleate at low temperature because of the dominant and rapid nucleation of the β form. At higher temperature, however, the kinetic energy of molecules at the substrate surface is higher, allowing nucleation of the energetically favorable γ form with better lattice matching on KCl and NaCl.

Concluding Remarks

The crystal structures and orientations of two polymorphic Ni(salen) crystals grown epitaxially on alkali halide substrates by vacuum deposition were investigated by HRTEM, HRED, and SAED. The crystal structures of Ni(salen) were found to depend on the structure and temperature of the substrate. At low substrate temperature, only the needle-like β form was formed. At higher substrate temperature, however, the more favorable γ form with better lattice match to the substrate surface was produced. It is thus considered that the structural form produced is related to the rate of nucleation and growth of a particular polymorph rather than directly controlled by the substrate lattice structure. The present results suggest that to achieve precise control of the polymorphic structures of molecular crystals it is necessary to consider the dynamics of deposited molecules in addition to the static properties of the substrate surface. As direct analysis of such dynamic effects is difficult, advancement

(28) Calligaris, M.; Nardin, G.; Randaccio, L. *Coord. Chem. Rev.* **1972**, *7*, 385–403.
(29) Girichev, G. V.; Giricheva, N. I.; Kuzmina, N. P.; Levina, Yu. S.; Rogachev, A. Yu. *J. Struct. Chem.* **2005**, *46*, 813–823.

in molecular dynamics calculations will prove essential in the development of molecular devices.

The β- and γ-Ni(salen) may exhibit higher redox conductivity along the molecular columns than the known α form, and the correlation between molecules along a molecular column may be useful in amplifying molecular interactions for specific applications. Precise control of the polymorphic structures is thus expected to be important in future applications of molecular effects.

Supporting Information Available: X-ray diffraction data, packing models, simulated HRTEM image and HRTEM images (Figures S1–S7; PDF). This material is available free of charge via the Internet at http://pubs. acs.org.

CM7018789